Colloid Polym Sci 274:568–575 (1996)

ORIGINAL CONTRIBUTION

M. Odenwald
H.-F. Eicke
Chr. Friedrich

Rheological analysis of triblock copolymer-microemulsion networks

Received: 6 September 1995
Accepted: 23 November 1995

M. Odenwald · Prof. Dr. H.-F. Eicke (✉)
Institut für Physikalische Chemie
Universität Basel
Klingelbergstraße 80
4056 Basel, Switzerland

Chr. Friedrich
Freiburger Materialforschungszentrum
Universität Freiburg
Stefan-Meier-Straße 31
79104 Freiburg

Abstract The rheological properties of microemulsion-triblock copolymer [poly(oxyethylene)-b-polyisoprene-b-poly(oxyethylene)] networks were studied by oscillatory shear measurements. The principal viscoelastic pattern of our systems stays the same whether the surfactant is ionic or nonionic. A closer examination shows, however, the enormous influence of the respective phase behavior of the underlying microemulsions. Also, specific interactions between the surfactants and the hydrophilic poly(oxyethylene) blocks lead to a significant effect on the formation of network structures. Characteristic rheological data such as plateau moduli and relaxation times for a series of different samples were derived differing in polymer or droplet concentrations, apart from the molecular weights of the poly(oxyethylene) and the polyisoprene blocks. Finally, we could construct polymer and droplet concentration invariant master – mastercurves using the temperature invariant mastercurves.

Key words Microemulsions – networks – blockcopolymers – dynamics – rheology

Introduction

Thermodynamically stable water-in-oil microemulsions consist (in a certain range of their phase diagrams) of *nano*meter-sized water *droplets* covered by a monomolecular surfactant layer in an oil continuum [1]. We report on ionic microemulsions formed by sodium bis(2-ethylhexyl) sulphosuccinate (= 'AOT')/water/isooctane and on nonionic microemulsions formed by pentakis(ethylene glycol)-mono(tetradecylether) ($C_{14}E_5$)/water/*n*-octane. The number (n) and diameter (d) of the aqueous nanodroplets are determined by weighed-in amounts of surfactant, water and oil. Typical values for the microemulsions are $d = 1.5 \cdot 10^{-8}$ m and $n = 3.9 \cdot 10^{16}$ cm^{-3}.

Their compartmental structure favors water-in-oil microemulsions to be "complex solvents" for ABA-triblock copolymers containing hydrophilic poly(oxyethylene) blocks (POE) and a lypophilic polyisoprene midblock (PI). While dissolving such block copolymers in w/o-microemulsions three-dimensional transient networks are formed above a certain polymer concentration [2, 3]. In these networks the aqueous nanodroplets form the network crosslinks incorporating the hydrophilic POE blocks and the oil soluble PI midblocks act as crosslinkers by bridging the nanodroplets (see Fig. 1).

From previous work [4] we know that water-in-oil microemulsions interact in a characteristic manner with ABA-triblock copolymers depending on the chemical nature of the surfactant, i.e., ionic or nonionic. Especially the exchange of hydrophilic POE blocks as constituents of crosslinks within the transient network, and thus the viscoelastic properties of our systems are essentially determined by the microemulsion's composition.

It appears interesting to elucidate how variations of other parameters, i.e., the concentrations of the block

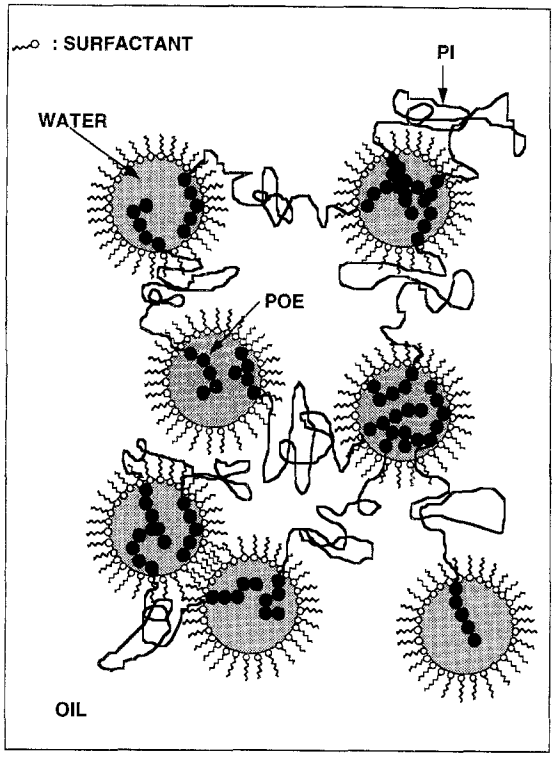

Fig. 1 Triblock copolymers forming a transient network in a water-in-oil microemulsion

copolymers or of the nanodroplets and the molecular weights of the individual blocks influence the dynamic properties. In this paper we report on transient networks formed by $C_{14}E_5$/water/*n*-octane (nonionic system, "nio") and AOT/water/isooctane (ionic system, "io") microemulsions containing [poly-(oxyethylene)-b-polyisoprene -b-poly-(oxyethylene)] triblock copolymers. Results of rheologic measurements on these systems are reported. From a theoretical point of view the dynamic properties of more simple systems, i.e., binary polymer–solvent mixtures forming transient networks, were already considered [5]. The present systems are remarkably more involved, hence there is no theoretical approach which could help to interpret the experimental data in this paper.

Experimental section

Material

Water-in-oil microemulsions contain the nonionic surfactant pentakis(ethylenglykol)-mono(tetradecyl ether) (= $C_{14}E_5$) or the ionic surfactant sodium bis(2-ethylhexyl) sulphosuccinate (= AOT). Both surfactants were obtained from Fluka at highest grade available and used without further purification, likewise *n*-octane and isooctane (puriss.). Water was deionized with an ALPHA-Q-Reagent Grade system from Millipore.

Table 1 [poly(oxyethylene)-b-polyisoprene-b-poly(oxyethylene)] blockcopolymers

Polymer	M_w (PI) [g/mol]	M_w (PEO) [g/mol]	M_w/M_n
TBC 6	50000	10000	1015
TBC 8	50000	5000	1015
COP 3	39000	11000	103

All three [poly(ethylene oxide)-b-polyisoprene-b-poly (ethylene oxide)] triblock copolymers TBC 6, TBC 8 and COP 3 (see Table 1) were synthesized via anionic polymerization and characterized as described elsewhere (TBC 6 and TBC 8: [4f]; COP 3: [4c]).

The polymer containing microemulsions were prepared by mixing weighed amounts of microemulsions with varying amounts of polymers and stirring the mixtures at 35 °C (io) or 20 °C (nio) for several days to ensure complete dissolution of the polymers. Mass fractions of the droplets, c_w, are given by

$$c_w = \frac{m_s + m_w}{m_s + m_w + m_o}, \tag{1}$$

with $m_x \cong$ mass of surfactant ($x = s$), water ($x = w$) and oil ($x = o$). Another parameter determined by c_w is the average shell-to-shell distance between two nanodroplets, δ (scaling of δ with c_w is shown in Fig. 6). The droplet diameter d is determined by the water/surfactant ratio

$$r_w = \frac{m_w}{m_s} \tag{2}$$

if ideal mixing is presumed.

The amount of polymer is given by the number ratio $R \cong$ (polymer molecules/ water droplet). For a microemulsion with $c_w = 0.20$ and $r_w = 2.50$ the mass concentrations of POE in the water droplets ranged from 8.94 mg ($R = 2$) to 89.40 mg ($R = 20$) (TBC8) and from 33.3 mg ($R = 3$) to 222.0 mg ($R = 20$) (TBC6 and COP3) per cm^3 H_2O. The mass concentrations of PI in the oil continuum ranged from 5.50 mg ($R = 2$) to 55.0 mg ($R = 20$) (TBC6 and TBC8) and from 9.50 mg ($R = 4$) to 28.5 mg ($R = 12$) (COP3) per cm^3 oil at highest c_w. The overlap concentration c^* of POE in water is given by either $c^* = 55$ mg/cm^3 or 67 mg/cm^3, for PI in isooctane we get $c^* = 41$ mg/cm^3 [6]. So we can suppose the PI being in the slightly dilute state, whereas the POE concentration reaches c^* at $R = 20$ (TBC8) and at lower polymer content ($R = 6$) for TBC6 and COP3. Compositions of the samples are listed in Table 2.

Table 2 Composition of the triblock copolymer-microemulsion systems. The r_w-value was 2.50 for all samples

Sample	Surfactant	Polymer	R	c_w
A 1	AOT	TBC 6	3	0.35
A 2	AOT	TBC 6	4	0.35
A 3	AOT	TBC 6	6	0.35
A 4	AOT	TBC 6	8	0.35
A 5	AOT	TBC 6	12	0.35
A 6	AOT	TBC 6	20	0.35
B 1	AOT	TBC 6	4	0.20
B 2	AOT	TBC 6	8	0.20
B 3	AOT	TBC 6	12	0.20
B 4	AOT	TBC 6	20	0.20
C 1	AOT	TBC 8	8	0.20
C 2	AOT	TBC 8	12	0.20
C 3	AOT	TBC 8	20	0.20
D 1	AOT	TBC 8	4	0.35
D 2	AOT	TBC 8	8	0.35
D 3	AOT	TBC 8	12	0.35
D 4	AOT	TBC 8	20	0.35
E 1	AOT	COP 3	4	0.20
E 2	AOT	COP 3	6	0.20
E 3	AOT	COP 3	8	0.20
E 4	AOT	COP 3	12	0.20
F 1	AOT	TBC 8	8	0.10
F 2	AOT	TBC 8	8	0.124
F 3	AOT	TBC 8	8	0.15
F 4	AOT	TBC 8	8	0.274
F 5	AOT	TBC 8	8	0.35
X 1	$C_{14}E_5$	TBC 8	3	0.20
X 2	$C_{14}E_5$	TBC 8	4	0.20
X 3	$C_{14}E_5$	TBC 8	6.2	0.20
X 4	$C_{14}E_5$	TBC 8	8	0.20

Measurements

In order to evaluate the dynamical properties of microemulsion-triblock copolymer systems rheological measurements were performed. They were carried out with a Carrimed CRSH 100 controlled stress rheometer, combined with a homemade cone-cone geometry ($3.5 \cdot 10^{-5}$ m gap, corrected for thermal expansion) and a thermostatable cap ($\pm$ 0.05 K) to isolate samples from outer atmosphere and prevent solvent evaporation (detailed description see [4e]). The rheometers transducer is sensitive down to a torque of 1 μNm.

Material functions, i.e., storage modulus $G'(\omega)$ and loss modulus $G''(\omega)$ were measured in the frequency range $0.628\ s^{-1} \leq \omega \leq 251.3\ s^{-1}$ at various temperatures, strain amplitudes of 1×10^{-3} rad and torques between 1 μNm and 900 μNm. The relative narrow frequency range had to be chosen to accelerate measurements because of limited sample stability in the rheometer. In Fig. 2 the courses of G' and G'' of an ionic sample ($R = 12$) are shown during a time sweep at $T = 18\,°C$ and $\nu = 1$ Hz. From this figure it can be clearly seen that the sample composition is constant only for about 1 h because the measuring unit could not be tightened completely in spite of all efforts.

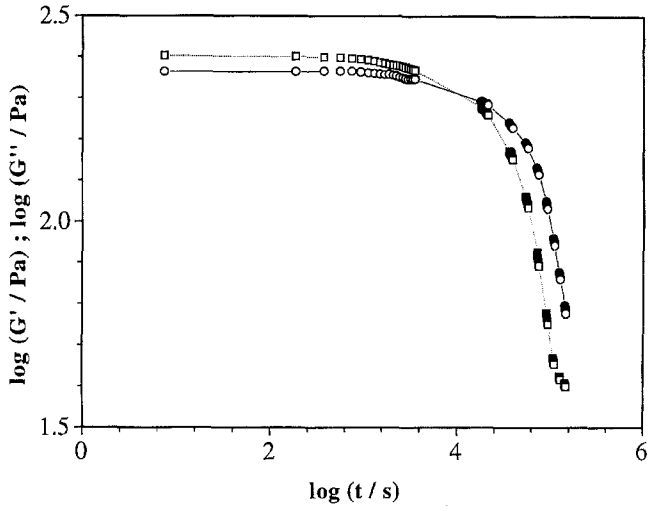

Fig. 2 Time sweep ($\nu = 1$ Hz, $T = 18\,°C$) to illustrate limited stability of an ionic microemulsion sample (polymer concentration: $R = 12$); (—○—) G', (··· □ ···) G''

All rheological measurements were carried out in the one-phase regions of the samples. Their temperature ranges are mostly determined, among other things, by the chemical nature of the surfactant. Due to this inevitable shift of the phase regions it was not possible to work with the same reference temperature for both systems, ionic and nonionic, while constructing the master curves (see "Results and Discussion").

Results and discussion

From previous work [4f] we know that the influence of the underlying microemulsions on the dynamical properties of the transient networks can be understood by considering their temperature-dependent phase behavior: it is well known that temperature variation causes reversible nanodroplet aggregation in microemulsions, eventually resulting in the formation of an infinite cluster of nanodroplets. The tendency of individual water globules (of given size and concentration) to aggregate is raised with increasing temperature for microemulsions stabilized by ionic surfactants. It is essential to note that this phase behavior is virtually preserved for the cross-linked systems containing block copolymers [7]. The network cross-links are formed by nanodroplets and their solubilized POE blocks while the oil soluble PI-blocks are connecting the droplets (see Fig. 1). Two effects can be anticipated if nanodroplets form clusters: approaching the infinite cluster transition temperature (T_c) the lifetime of droplet–

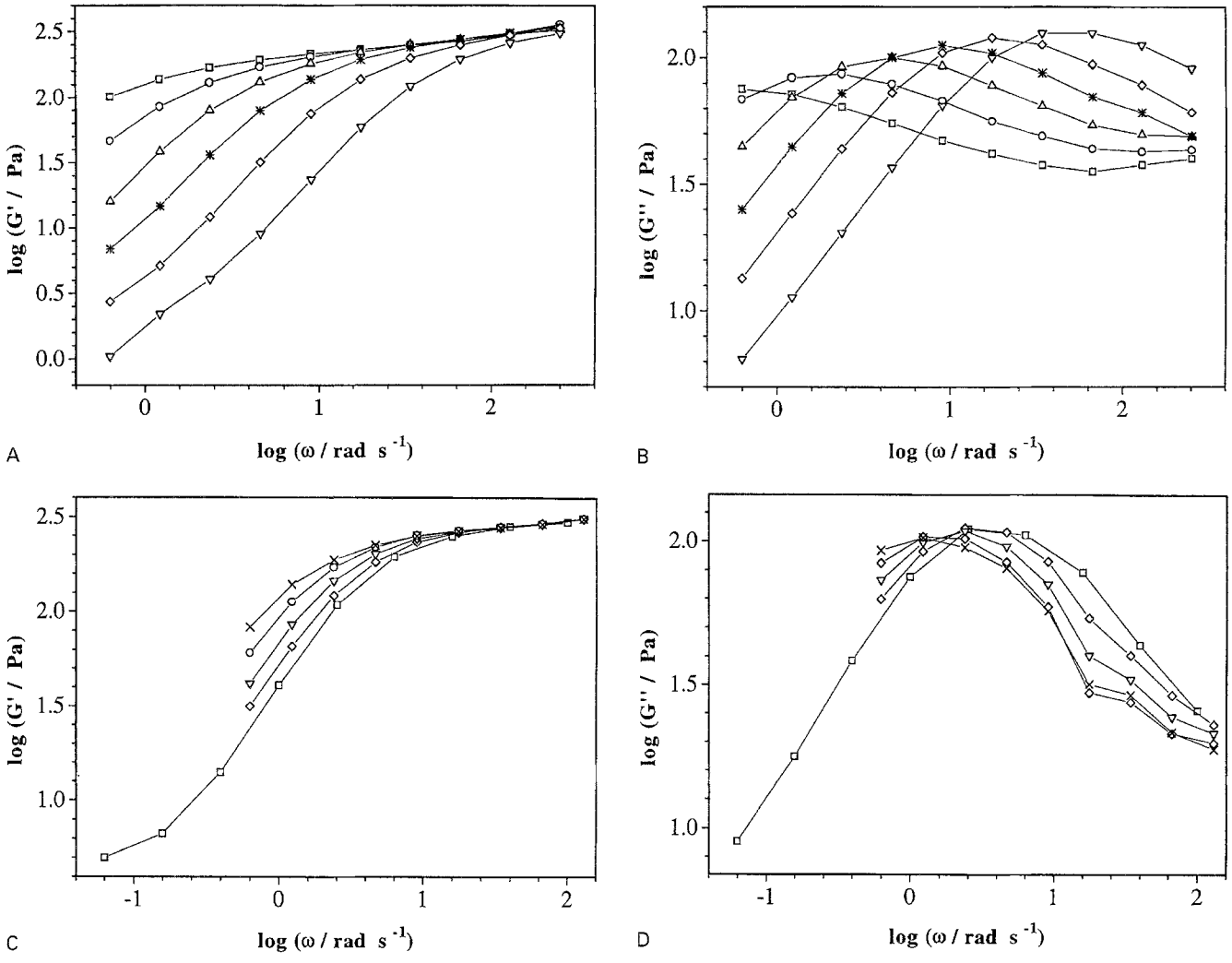

Fig. 3A Storage moduli of the sample B 3; (□) 278 K, (○) 280.5 K, (△) 283 K, (*) 285.5 K, (◇) 288 K, (▽) 291 K, **B** Loss moduli of the sample B 3; (□) 278 K, (○) 280.5 K, (△) 283 K, (*) 285.5 K, (◇) 288 K, (▽) 291 K, **C** Storage moduli of the sample X 4; (□) 301 K, (◇) 304 K, (▽) 305 K, (○) 306 K, (X) 307 k, **D** Loss moduli of the sample X 4; (□) 301 K, (◇) 304 K, (▽) 305 K, (○) 306 K, (×) 307 K

droplet contact grows. This favors the exchange of POE blocks between nanodroplets and, consequently, lowers the lifetime of a single network cross-link. Moreover, the formation of droplet clusters disturbs the structure of the whole transient network [4f].

Ionic w/o-microemulsions containing triblock copolymers behave similar to common polymer solutions under oscillatory shear. This is seen from the isotherms of both material functions, i.e., storage modulus $G'(\omega)$ and loss modulus $G''(\omega)$ of a sample with $R = 8$, $c_w = 0.20$ and $r_w = 2.50$ in Figs. 3A and 3B. At a fixed frequency the storage modulus decreases with raising temperature verifying that the sample adopts a more viscous and a less elastic behavior.

If the nonionic surfactant $C_{14}E_5$ replaces the ionic surfactant AOT the viscoelastic behavior of the triblock copolymer mediated nonionic microemulsions was, qualitatively, the same as documented by the isotherms of a nonionic sample in Figs. 3C and 3D. In nonionic microemulsion systems $G'(\omega)$ raises with increasing temperature at fixed frequency. The reason for this is the nonionic microemulsions' phase behavior where the nanodroplets, clustering at lower temperatures, become increasingly dispersed with rising temperature within the one phase region of the system.

Using the isotherms we can construct master curves with respect to the reference temperatures $T_{ref} = 18\,°C$ (ionic) and $T_{ref} = 30\,°C$ (nonionic). The dynamic material functions $(b_T \cdot G')$ and $(b_T \cdot G'')$ are plotted as functions of the reduced frequency $(a_T \cdot \omega)$ for different polymer concentrations but the same compositions of the ionic and nonionic microemulsions ($c_w = 0.20$ and $r_w = 2.50$) in

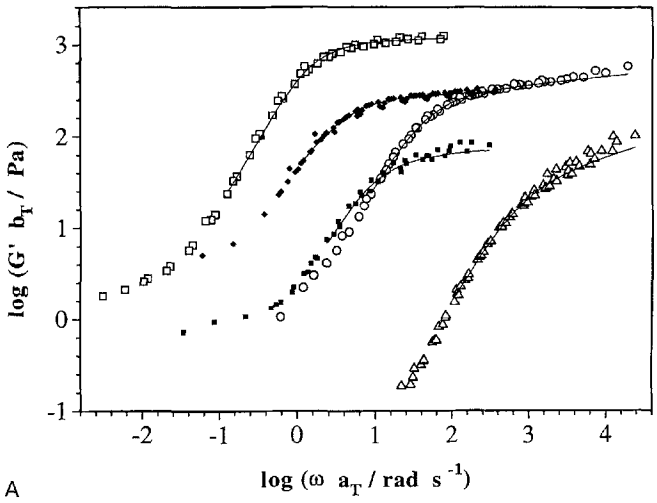

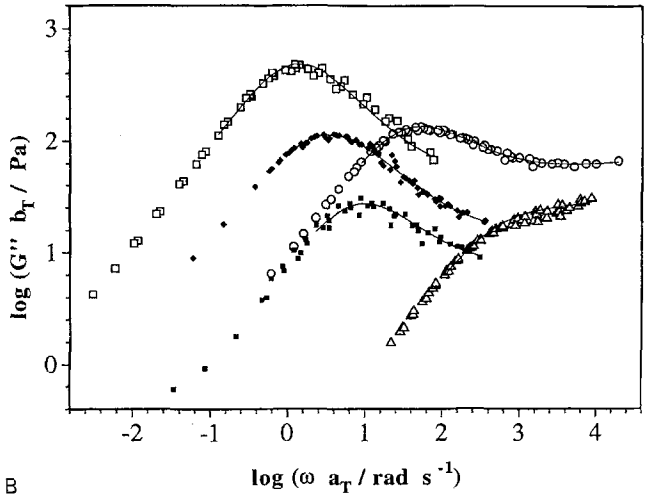

Fig. 4A Master curves of storage moduli of the series B (ionic, $T_{ref} = 18\,°C$) and X (nonionic, $T_{ref} = 30\,°C$); (□) B 4, (○), B 3, (△) B 2, (◆) X 4, (■) X 2. (—) Fit corresponding to Eq. (4), **B** Master curves of loss moduli of the series B (ionic, $T_{ref} = 18\,°C$) and X (nonionic, $T_{ref} = 30\,°C$); (□) B 4, (○), B 3, (△) B 2, (◆) X 4, (■) X 2. (—) Fit corresponding to Eq. (5)

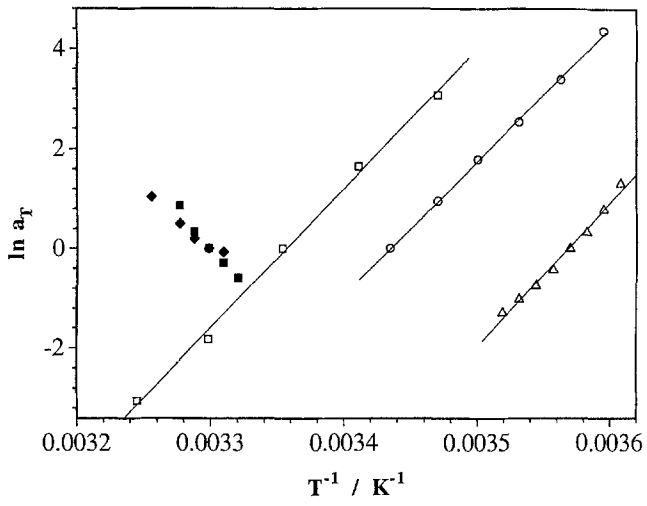

Fig. 5 Arrhenius plots of the horizontal shift factors a_T used to construct the mastercurves of Figs. 4A and 4B; (□) B 4, (○), B 3, (△) B 2, (◆) X 4, (■) X 2. Straight lines represent linear regressions

Figs. 4A and 4B. These master curves are typical examples for the dynamical properties of our systems. There exist two relaxation processes, the first one is observed at higher frequencies, whereas the second one occurs in the low frequency region of each master curve. A better discrimination of this second relaxation process was impossible because of equipment limitations which prevented one to observe G_{P_2} at lower polymer concentrations (torques fall short of transducers' of low limit 1 μNm); at higher R-values the flow region could not be attained (required measuring times were larger than sample stability of about 60 min in the rheometer). Finally, G_{P_2} (low freq. plateau modulus) cannot be an equilibrium modulus as considered in permanent networks. In our samples a viscous flow can be observed even at highest polymer concentrations and at rather low temperatures. Because of experimental difficulties described above we focus on the first, clearly detectable, high frequency relaxation process and do not discuss the second one at lower frequencies. Concerning the influence of the polymer concentration on the dynamical properties we see from Fig. 4A that the plateau modulus G_{P_1} of the high frequency relaxation process raises with increasing R as does the corresponding relaxation time τ_{m_1}. Nevertheless, this process cannot be classified as a classical terminal relaxation because the slopes of G' and G'' differ from theoretical predictions 2 and 1 and an additional low frequency relaxation process shows up with plateau modulus G_{P_2} and relaxation time τ_{m_2}.

The time-temperature superposition principle is valid for our systems within the observed temperature regions. For the horizontal shift factors a_T an Arrhenius-like temperature dependence

$$a_T = \exp\left[-\frac{E_A}{R}\cdot\left(\frac{1}{T_{ref}}-\frac{1}{T}\right)\right] \tag{3}$$

was found to be appropriate for all ionic microemulsions as shown in Fig. 5 (the WLF-equation did not yield satisfactory results). The a_T plot of a nonionic sample shows the inverse temperature dependence; values of the vertical shift factors, b_T, scattered around 1 as one could expect for the measurable small temperature ranges. The high frequency relaxation process in ionic systems is characterized by the activation energies E_A. The latter are plotted against the average distance δ between the shells of two aqueous nanodroplets (Fig. 6); in the same figure the dependence of

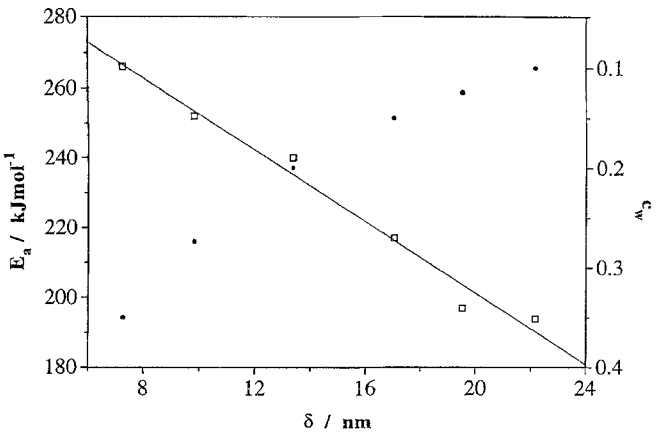

Fig. 6 Activation energies in dependence of δ obtained from Arrhenius plots of series F (□). Concentration of nanodroplets c_w in dependence of δ(•) . Straight line represents linear regression

δ on c_w is shown. This plot establishes a linear dependence of E_A on δ (which is in good agreement with earlier data of our group [4e]). Also, it is fairly independent of other parameters of our ionic systems, i.e., polymer concentration and molecular weights of both blocks, i.e., poly(oxyethylene) and polyisoprene. At first sight it may seem surprising that E_A decreases with growing δ. This feature can be explained, however, with the molecular picture established in earlier papers [8]; the PI-midblocks bridge the oil phase between two nanodroplets. The existence of a viscoelastic plateau modulus G_{P_1} indicates that a certain amount of energy E_{el} is stored elastically within this midblock. The larger the average distance between the shells of two different nanodroplets, the more extended is the midblock and hence it stores a larger amount of E_{el}; less activation energy has to be brought up, therefore, for the disruption of POE-endblocks from nanodroplets.

In microemulsion-triblockcopolymer networks we have to distinguish two possible mechanisms determining the lifetime of network cross-links in the experimentally accessible temperature region: exchange of POE blocks ($\cong$ network links) between nanodroplets i) across the surrounding oil phase and ii) during collision of two nanodroplets [4f]. As long as viscoelastic behavior is controlled by the disruption of POE blocks from nanodroplets associated with mechanism i), an Arrhenius-like temperature dependence should be observed. In the ionic systems we detect such a temperature dependence relative to the high frequency relaxation process because attractive interactions between the ionic surfactant head groups and the POE-chains let the mechanism i) occur at shorter time scales than ii). This mechanism i) turns out to control the first relaxation process at high frequencies in ionic microemulsions. Opposite, in nonionic systems mechanism ii) dominates within the observed time scale. Because of repulsive interactions between the POE-blocks and the nonionic surfactant it is very difficult for the POE-blocks to cross the oil phase as described by mechanism i). Therefore, it is not possible to find characteristic activation energies as for ionic systems described above.

An empirical rheological constitutive equation [9] modelling generalized Cole–Cole behavior allowed us to calculate the material functions $G'(\omega)$ and $G''(\omega)$ of the high frequency relaxation process and thus to determine G_{P_1}, τ_{m_1} and the slopes in the power law region:

$$G' = G_{P_2} + (G_{P_1} - G_{P_2}) \cdot (\omega\, \tau_{m_1})^{\beta} \cdot \frac{[\cos(\frac{\beta}{2}\pi) + (\omega\, \tau_{m_1})^{\alpha} \cos(\frac{\beta-\alpha}{2}\pi)]}{1 + 2(\omega\, \tau_{m_1})^{\alpha} \cos(\frac{\alpha}{2}\pi) + (\omega\, \tau_{m_1})^{2\alpha}} \quad (4)$$

$$G'' = (G_{P_1} - G_{P_2}) \cdot (\omega\, \tau_{m_1})^{\beta} \cdot \frac{[\sin(\frac{\beta}{2}\pi) + (\omega\, \tau_{m_1})^{\alpha} \sin(\frac{\beta-\alpha}{2}\pi)]}{1 + 2(\omega\, \tau_{m_1})^{\alpha} \cos(\frac{\alpha}{2}\pi) + (\omega\, \tau_{m_1})^{2\alpha}} \quad (5)$$

with α, $\beta \cong$ power law exponents controlling the slopes of the material functions in both power law regions.

Equations. (4) and (5) degenerate to the well known Cole–Cole model as presented and discussed by Tschoegl [10] under the condition $\alpha = \beta$. The results of the calculations are plotted in Fig. 7A (G_{P_1}) and Fig. 7B (τ_{m_1}) for different systems as functions of R (the dotted lines are guidelines to the eyes) and for constant polymer concentration ($R = 8$) as functions of the interdroplet distance δ (Fig. 7C).

From all plots of Fig. 7A it is evident that G_{P_1} increases with increasing R in a similar manner. This corresponds to an increase of the "functionality" of the crosslinks and of the samples' viscosities since increasing amounts of triblock copolymers are dissolved in the microemulsion. A change of molecular weight of the PI-midblock yields lower plateau moduli for longer PI-chains which is in qualitative agreement with the classical network theory: the storage modulus scales with the reciprocal molecular weight of the polymer chains between two network crosslinks [11]. The triblock copolymer with POE-blocks of 10.000 g/mol yields higher G_{P_1} than POE-blocks of 5.000 g/mol. Finally, G_{P_1} depends linearly on δ (Fig. 7C). A decrease of δ is equivalent to an increase of the density of network crosslinks with constant functionality. The comparison between ionic and nonionic systems shows that in case of nonionic surfactant G_{P_1} reaches much larger values at the same polymer content, e.g., G_{P_1} is by almost one decade larger in series X than in series C at $R = 8$ (see Fig. 7A). This feature cannot be explained yet.

The second characteristic of the high frequency relaxation process is the relaxation time τ_{m_1}. Similar to G_{P_1} the

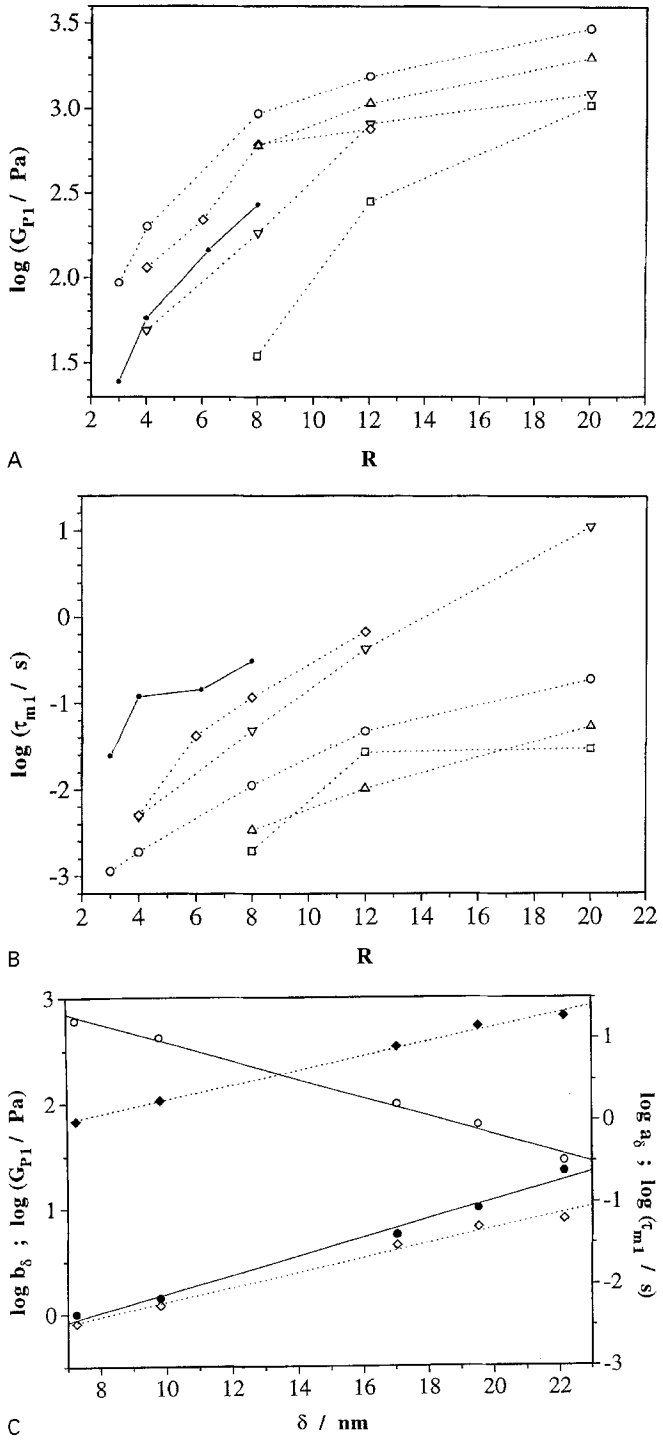

Fig. 7A High frequency plateau moduli G_{P_1} plotted against polymer concentration R for different series: (○) series A; (▽) series B; (□) series C; (△) series D; (◇) series E; (○) series X. Straight and dotted lines are guides for the eye, **B** High frequency relaxation time τ_{m_1} plotted against polymer concentration R for different series: (○) series A; (▽) series B; (□) series C; (△) series D; (◇) series E; (●) series X. Straight and dotted lines are guides for the eye, **C** High frequency relaxation process parameters τ_{m_1} (◇), G_{P_1} (○) and shift factors a_δ (◆), b_δ (●) plotted against interdroplet distance δ for series F. Straight and dotted lines represent linear regressions

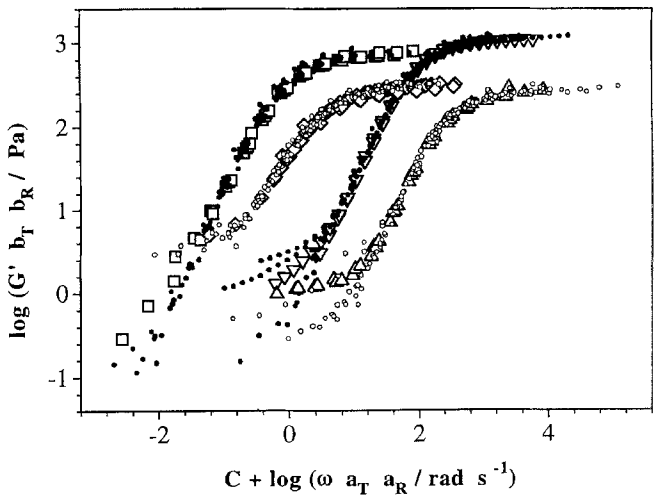

Fig. 8 Temperature and R invariant master-mastercurves. Open and filled small circles: temperature invariant mastercurves of the corresponding series A, B, C and X (see Table 2) shifted with respect to $R_{ref} = 8$ (large open symbols): (▽) A4; (△) B2; (□) E3; (◇) X4. To spread the x-axis a shift constant C was added to two of the master-mastercurves: series B ($C = +2$); series E ($C = -1$)

high frequency relaxation time is increasing with growing polymer content in all series as shown in Fig. 7B. Variation of R and the doubling of the POE – block length affects τ_{m_1} strongly in ionic systems, while variation of the PI-block has only a minor effect. The main reason for this might be seen in exceeding the overlap concentration c^* for the POE-blocks of 10 000 g/mol even at low R. The shorter POE-blocks (5 000 g/mol) do not reach c^* until $R = 20$. Thus we can infer that the large differences of the high frequency relaxation times between both kinds of POE stem from a hindrance of POE-disruption by the overlapping of the larger endblocks. In Fig. 7C the linear increase of τ_{m_1} with larger interdroplet distances δ is shown.

The exchange of nonionic by ionic surfactant induces a dramatic increase of τ_{m_1} at constant R and δ. In the nonionic system the values of τ_{m_1} are largest (Fig. 7B) even for short POE-blocks and a T_{ref} of 30 °C (ionic systems: 18 °C). This is another hint in favor of the repulsive interactions between the nonionic surfactant and the POE-blocks and, therefore, for the dominating mechanism ii) regarding the POE-exchange [9]. This mechanism occurs on a much longer time scale than mechanism i) as discussed before.

Finally, it was possible to create so-called master-mastercurves with respect to the first relaxation process and a reference polymer concentration of $R_{ref} = 8$ using the R-dependent mastercurves of the single microemulsion series A to E. Figure 8 shows examples of such temperature and polymer concentration invariant master-

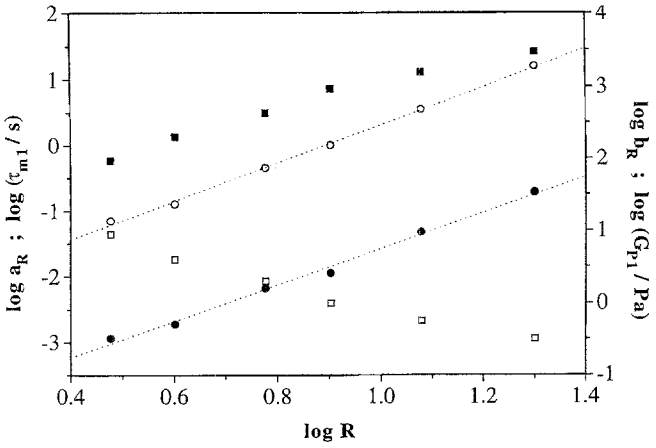

Fig. 9 Horizontal shift factors a_R (○), vertical shift factors b_R (□) used for constructing the supermastercurve of series A in Fig. 8 and corresponding τ_{m_1} (●), G_{P_1} (■). Dotted lines represent linear regressions

mastercurves. In the same way the F series with varying c_w could be shifted onto a reference interdroplet distance $\delta_{ref} = 7.27$ nm or $c_w = 0.35$, respectively. The results of the calculations following Eqs. (4) and (5) allowed to construct these master-mastercurves because values of the slopes α and β of the material functions were in the range of $0.89 \leq \alpha \leq 0.94$ and $0.89 \leq \beta \leq 1.00$ for all single temperature invariant master curves. Obviously, the horizontal and vertical shifts of the high and low frequency relaxation processes follow different scaling laws.

Shift factors $\log a_R$ and $\log b_R$ of series A as an example for all R-invariant master-master curves are plotted together with $\log \tau_{m_1}$ and $\log G_{P_1}$ against $\log R$ (Fig. 9). The horizontal shift factors a_R and τ_{m_1} depend linearly on R, while the vertical shift factors b_R and G_{P_1} are still nonlinear with R.

A similar representation for the F series is included in Fig. 7C. In this case both shift factors, i.e., horizontal a_δ and vertical b_δ, depend linearly on the interdroplet distance δ as do the corresponding parameters of the high frequency relaxation process, i.e., τ_{m_1} and G_{P_1}.

Conclusions

We obtained an interesting collection of detailed rheologic data. They could be related to molecular processes in transient networks formed by triblock copolymers dissolved in ionic and nonionic water-in-oil microemulsions. Such processes are believed to be responsible for the viscoelastic behavior of these complex materials. The feasibility of constructing polymer or nanodroplet concentration invariant master-mastercurves for all systems investigated leads to the assumption that there is a common overall dynamic process at higher frequencies which results from polymer-nanodroplet interaction. In contrast, the low frequency relaxation process tracing larger network clusters follows different scaling laws. To study the respective frequency range requires material with a sufficient stability in the rheometer which has to be much longer than that of the samples used in this work.

Acknowledgement The authors are grateful to Drs. W. Meier and F. Stieber for valuable discussions. They also acknowledge help with the experiments by H. Hammerich and Y. Hauger. This work was supported by the Swiss National Science Foundation.

References

1. a) De Gennes PG, Taupin C (1982) J Phys Chem 86:2294
   b) Jouffroy J, de Gennes PG (1982) J Phys (Les Ulis Fr) 43:1241
   c) Borkovec M, Eicke HF, Hammerich H, Das Gupta B (1988) J Phys Chem 92:206
2. a) Green MS, Tobolsky AV (1946) J Phys Chem 14:80
   b) Lodge AS (1964) Elastic Liquids, Academic Press, New York
3. a) Baxandall LG (1989) Macromolecules 22:1982
   b) Tanaka F (1990) Macromolecules 23: 3784
4. a) Eicke H-F, Quellet C, Xu G (1989) Colloids Surf 36:97
   b) Quellet C, Eicke H-F, Hauger Y (1990) Macromolecules 23:3347
   c) Eicke H-F, Hilfiker R, Xu G (1990) Helv Chim Acta 73:213
   d) Struis RPWJ, Eicke H-F (1991) J Phys Chem 95:5989
   e) Zölzer U, Eicke H-F (1992) J Phys II 2:2207
   f) Odenwald M, Eicke H-F, Meier W (1995) Macromolecules 28:5069
5. a) Bird RB, Armstrong RC, Hassager O (1987) Dynamics of polymeric liquids, J Wiley & Sons, New York
   b) Tanaka F, Edwards SF (1992) Macromolecules 25:1516
   c) Tanaka F, Edwards SF (1992) J Non-New Fluids Mechanics 43:247–309
6. Fleischer G, Stieber F, Hofmeier U, Eicke H-F (1994) Langmuir 10:1780 and references cited therein
7. a) Lagues M, Ober R, Taupin C (1978) Journal de physique-letters 39:L487–L491
   b) Eicke HF, Hilfiker R (1984) Helv Chim Acta 67/2:361–372
8. Meier W, Odenwald M, Fedtke B, Eicke H-F (1994) presented at the 5th European Polymer Federation Symposium On Polymeric Materials (EPF), Basel (Switzerland)
9. a) Brochard-Wyart F, de Gennes PG, Léger L, Marciano Y, Raphael E (1994) J Phys Chem 98:9405
   b) Raphael E, de Gennes PG (1992) J Phys Chem 96:4002
10. Friedrich C, Braun H (1992) Rheol Acta 31:309
11. Tschoegl NW (1989) The Phenomenological Theory of Linear Viscoelastic Behavior, Springer-Verlag, Berlin
12. Flory PJ (1953) Principles of Polymer Chemistry, Cornell University Press, Ithaca, pp 432 ff